

THE ARECIBO FAST RADIO BURST: DENSE CIRCUM-BURST MEDIUM

S. R. KULKARNI¹, E. O. OFEK² & J. D. NEILL³

Draft of July 25, 2018

ABSTRACT

The nature of fast radio bursts (FRB) showing a single dispersed few-ms-width pulse, with dispersion measure (DM) in excess of the Galactic value has been extensively debated. Here we investigate FRB 121102, the first FRB detected at the 305-m Arecibo radio telescope and remarkable for its unusually large spectral index. After extensive explorations of options we conclude that the spectral index is caused by a nebula with free-free absorption. Observations (or lack thereof) show that the nebula is located beyond the Milky Way. We conclude that FRBs are of extra-galactic origin and that they arise in dense star-forming regions. The challenge with extra-galactic models is the the high volumetric rate of FRBs. This high rate allows us to eliminate all forms of catastrophic stellar death as a progenitor. Hyper-giant flares from young magnetars emerge as the most likely progenitors. A number of consequences follow from this hypothesis: (i) FRB models which posit a purely intergalactic origin can be safely ignored. (ii) The rich ISM environment of young magnetars can result in significant contribution to DM, Rotation Measure (RM) and in some cases to significant free-free optical depth. (iii) The star-forming regions in the host galaxies can contribute significantly to the DM. Including this contribution reduces the inferred distances to FRBs and correspondingly increases the volumetric rate of FRBs (and, in turn, may require that giant flares can also produce FRBs). (iv) FRBs are likely to be suppressed at lower frequencies. Conversely, searching for FRBs at higher frequencies (2–5 GHz) would be attractive. (v) The blast wave which produces the radio emission can undergo rapid deceleration if the circum-burst medium is dense (as maybe the case for FRB 121102), leading to X-ray, radio and possibly γ -ray emission. (vi) Galaxies with high star formation rate host will have a higher FRB rate. However, such FRBs will have differing DMs owing to differing local contributions. (vi) The DM and RM of FRBs will prove to be noisy probes of the intergalactic medium (density, magnetic field) and cosmography.

Subject headings: ISM: general – radio continuum: general – pulsars:general— galaxies

1. BACKGROUND

Fast Radio Bursts (FRBs) were first identified in an archival analysis of pulsar data obtained with a multi-beam receiver at the 64-m radio telescope of the Parkes Observatory and operating in the 1.4 GHz band (Lorimer *et al.* 2007). The few millisecond wide burst showed a quadratic frequency dependent arrival time similar to pulsar signals traversing the Galactic ionized interstellar medium (ISM). The inferred dispersion measure (DM) was greatly in excess of that expected from a Galactic source. A simple interpretation was that the burst of radiation came from another galaxy (or was located in intergalactic space) with the excess DM due to electrons in the intergalactic medium (IGM).

However, subsequently, “peryttons” – radio bursts, but appearing in many (all) beams – were discovered. Telescopes are focused for sources at infinity and so celestial sources typically occur in only one beam.⁴ In contrast, local sources appear in many beams. Thus, peryttons cast doubts about the celestial origin of FRBs. How-

ever, recently peryttons were shown to emanate from a microwave oven at the Parkes Observatory (Petroff *et al.* 2015). With peryttons firmly established to be of domestic origin the standing of FRBs has risen.

For FRB 010724, Kulkarni *et al.* (2014; hereafter, K14) considered the possibility of an intervening Galactic nebula to account for the DM in excess of that provided by the Galactic ISM. Such a nebula would shine via emission (recombination lines) and also absorb radio signals (via free-free absorption). No plausible nebula was identified within the localization region of FRB 010724.

To date there are fifteen FRBs reported from the Parkes Observatory (Keane & Petroff 2015; Ravi, Shannon & Jameson 2015; Champion *et al.* 2015)). This number would be doubled by including FRBs discussed in the hallways of astronomy departments. The typical peak flux density, S_p , at the fiducial frequency, $\nu_0 = 1.4$ GHz, is between 0.5 Jy to 2 Jy. The durations⁵ ($\Delta\tau$) range from 1 ms to 10 ms. FRB 010724 is the brightest to date with a fluence of $\mathcal{F} = S_p\Delta t$ of several hundred Jy ms and also has one of the lowest dispersion measures, $375 \text{ cm}^{-3} \text{ pc}$. The highest reported DM is about $1629 \text{ cm}^{-3} \text{ pc}$ (Champion *et al.* 2015). The overall daily all-sky rate is 2500 events with $\mathcal{F} \geq 2 \text{ Jy ms}$ (Keane & Petroff 2015) and $6_{-3}^{+4} \times 10^3$ for the entire detected Parkes sample (Champion *et al.* 2015).

The extra-galactic origin for FRBs, whilst very appeal-

¹ Caltech Optical Observatories 249-17 Caltech, Pasadena, CA 91125, USA

² Department of Particle Physics & Astrophysics, Weizmann Institute of Science, Rehovot 76100, Israel

³ Space Radiation Laboratory 290-17, Caltech, Pasadena, CA 91125, USA

⁴ FRB 010724, the super-bright event discovered by Lorimer *et al.* (2007), occurred in several beams. At times some FRBs, if located in between the sky positions of two beams, are found in adjacent beams.

⁵ Note that there is loss of sensitivity for sub-ms duration bursts

ing,⁶ has two great challenges (see K14 for further details). First FRBs, if extragalactic, would be as brilliant as the nanosecond pulses from pulsars except that FRBs last for a few milliseconds. The energy radiated in the radio alone would be an impressive 10^{40} erg. Next, assuming most of the inferred DM is due to electrons in the IGM, the volumetric rate of FRBs is an impressive ten percent of the core-collapse supernova rate. A key requirement for any model of FRBs is that the radio pulse has to be able to propagate. This means that the circum-burst density must be low enough that the resulting plasma frequency is lower than ν_0 . Next, the optical depth to free-free opacity should also not be prohibitively large. These requirements rule out all supernovae models (see K14). So the progenitors of FRBs come from (i) a new channel of stellar death or (ii) an entirely new channel of non-stellar phenomenon or (ii) some sort of repeating phenomenon. The first two possibilities would be revolutionary. The third possibility, whilst less alarming, would have to rise to the challenges posed by the duration and energetics of FRBs.

2. THE ARECIBO FAST RADIO BURST

FRB 121102 was found in an analysis of archival data (Spitler *et al.* 2014; hereafter, S14) obtained from the seven-beam receiver located at the Gregorian focus of the Arecibo 305-m radio telescope and operating in the 1225–1525 MHz band (Cordes *et al.* 2006). This event is noteworthy for being the first FRB detected outside the Parkes Observatory.

The specific pulsar survey targeted the Galactic anti-center and lasted 11.8 d. The burst was detected in beam number 4 of the multi-beam system with an SNR of 11 (integration time of 3 ms). The sky position of the center of beam 4 is $l = 174^\circ.95$ and $b = -0^\circ.223$ which corresponds to RA=05h32m9.6s & Declination=33d05m13s (J2000). No bursts were seen during subsequent observations of the same region of the sky.

The event lasted about 3 ms and exhibited a frequency-dependent arrival time, $t_a \propto \nu^m$ with $m = -2.01 \pm 0.05$, consistent with that expected for a signal propagating through cold plasma. The apparent DM is $557.4 \pm 2 \text{ cm}^{-3} \text{ pc}$. The pulse width appears to be independent of the frequency. After accounting for the spectrometer resolution, S14 determine the intrinsic pulse width is $\Delta\tau_d < 1 \text{ ms}$ at $\nu_0 = 1.4 \text{ GHz}$. The best fit spectral index⁷ is positive, $7 < \beta < 11$. This is a remarkable spectral index especially for coherent radio emission.⁸

The inference of the peak flux density, S_p , depends on the sky location of FRB 121102 with respect to the principal axis of beam 4. The gain of a feed is maximum along the principal axis and decreases with increasing angle. Sources can be detected outside the nominal “beam at half maximum” provided they are bright. The peak antenna temperature of FRB 121102 is about 0.28 K. If the event is located in the primary beam of beam 4 then $S_p = 0.04 \text{ Jy}$ which would make it the faintest FRB to

⁶ The diagnostic value of readily detectable millisecond pulses originating from cosmological distances is immense, perhaps even transformational.

⁷ Here, $S(\nu)$, the flux density at frequency ν is modeled as $S(\nu) \propto \nu^\beta$.

⁸ On good grounds we expect the fundamental mechanism of FRBs is some sort of coherent emission.

date. On the other hand, S14, noting the unusual spectral index, argue the source was detected in the side lobe. If so, $S_p \approx 0.4 \text{ Jy}$, not too different from those of FRBs detected at Parkes. In short, the fluence of FRB 121102 at the fiducial frequency, ν_0 , can be as small as 0.12 Jy ms or as large as 1.2 Jy ms .

FRB 121102 is located close to the Galactic Equator ($b \approx -0.22^\circ$) and towards the anti-center region ($l \approx 175^\circ$). According to S14, the Galactic ISM, if integrated to the edge of the Galaxy, would contribute a dispersion measure of about $188 \text{ cm}^{-3} \text{ pc}$. If FRB 121102 is extragalactic then the excess DM is about $370 \text{ cm}^{-3} \text{ pc}$.

S14 considered terrestrial origins as well as a Galactic origin (Rotating Radio Transients). They disfavor both these two possibilities. Noting that FRB 121102 shared many similarities with events found at the Parkes Observatory (Lorimer *et al.* 2007; Thornton *et al.* 2013) S14 enthusiastically joined their colleagues at Parkes in advocating an extra-galactic origin for FRB 121102.

2.1. Why is FRB 121102 interesting?

In the short history of FRBs, FRB 121102 occupies a special position. We have already noted the remarkable spectral index. Next, given the detection of this event in a single Arecibo beam, is that FRB 121102 has to lie beyond the Fresnel length or about 100 km away from the telescope. These two observations provide unique insights into the origin of FRBs and provide the motivation for this paper.

The structure of the paper is as follows. The two unique attributes of FRB 121102 are discussed in §3 and §4. We explore several possibilities to account for the spectral index and conclude that the large positive spectral index is due free-free absorption arising in an inter-vening ionized clump (nebula). The locale of this putative nebula (galactic, extra-galactic, circum-FRB) are explored in §5–§7. In §8 we present our “best-buy” model, namely that FRBs are powered by (hyper) giant flares from young Soft Gamma-ray Repeaters (SGRs). This model accounts for the apparent fecundity of FRBs as well as provides a most natural explanation for the peculiar spectral index. We end the paper by discussing the considerable ramifications of this model (§9).

3. THE MINIMUM DISTANCE TO FRB 121102

Radio telescopes are tuned to receive signals from sources very far away (Fraunhofer regime). Thus, “nearby” (local) sources are expected to be out of focus and appear in several beams (e.g., perytons). The “single beam” criterion is usually interpreted to mean that the event is at a great distance from the telescope. The Fresnel length scale, a_F , separates nearby sources from very distant sources. It is given by⁹

$$a_F = \frac{\mathcal{D}^2}{4\lambda} \quad (1)$$

where \mathcal{D} is the diameter of the telescope and $\lambda = c/\nu$ is the wavelength. The Fresnel number is

$$n_F = a_F/d \quad (2)$$

⁹ Note that the expression for a_F in K14 is off by a factor of 4. The Fresnel scale is the ratio of the square of the radius to the wavelength.

where d is the distance to the source. Sources which are within a few Fresnel scales or with Fresnel number greater than one can be considered as nearby (technically, “near-field”). In Figure 1 we plot the beam response of an idealized radio telescope. From this we see that sources with $n_F > 1.5$ could be detected in adjacent beams (assuming tightly packed beams).

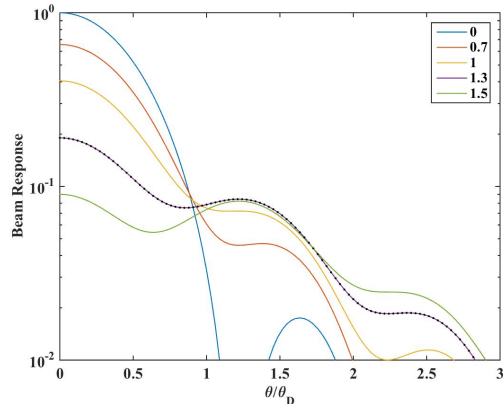


FIG. 1.— The beam response of a circular aperture illuminated uniformly for a point source located at a distance $d = a_F/n_F$ as a function of the Fresnel number, n_F (whose values can be found in the legend box). The angular offset is units of the diffraction angle, $\theta_D = \lambda/\mathcal{D}$ where \mathcal{D} is the diameter of the aperture. The response is normalized to unity for point source which is along the principal axis of the aperture and located at infinity.

For the Parkes telescope, $a_F \approx 5$ km at $\lambda = 21$ cm. In contrast, for the 305-m Arecibo dish, $a_F \approx 110$ km. Since Arecibo is a transit telescope sources are only found at high elevation angles. Thus, the detection of FRB 121102 in a single beam at Arecibo implies that FRBs cannot be located in the troposphere nor the stratosphere and perhaps even the mesosphere.¹⁰ Given the torturous history of FRBs it is not unreasonable to consider the possibility that FRBs may arise from some domestic or otherwise utensil on the International Space Station.¹¹ However, the very low declination (-75°) of the very first event, FRB 010724 rules out this proposal.

The next possibility is that FRB 121102 arises in the solar system¹². However, the authors lack the imagination and knowledge to consider this possibility. So going forward, we will only consider the following three possibilities for the origin of FRB 121102:

- (i.) FRB 121102 (and by implication the Parkes FRBs) is an ionospheric event.
- (ii.) FRB 121102 is Galactic event.¹³
- (iii.) FRB 121102 (and by implication the Parkes FRBs) are extra-galactic events.

¹⁰ The structure of the atmosphere, starting at sea level, is as follows: the troposphere (edge at 12 km); the stratosphere (45 km); the mesosphere (85 km); the ionosphere (1000 km).

¹¹ Near circular orbit with height of 410 km and inclination of $51^\circ.65$.

¹² This suggestion is motivated by a paper by Karbelkar (2014). It is worth noting that the ecliptic latitude of FRB 121102 is $9^\circ.8$.

¹³ We allow for this possibility since the spectrum of FRB 121102 is peculiar when compared to that of the Parkes FRBs.

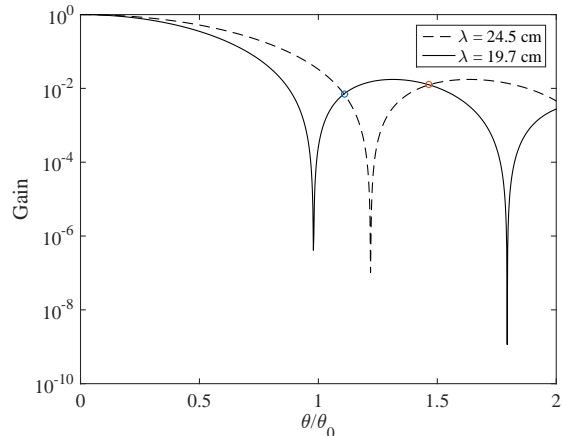


FIG. 2.— The beam response for a point source with spectral index, $\alpha = 0$, for an unobstructed feed as a function of θ/θ_D where $\theta_0 = \lambda_0/\mathcal{D}$ with $\lambda_0 = 21$ cm; as in the text, \mathcal{D} is the diameter of an unobstructed circular aperture. The beam response is shown for $\lambda = 19.7$ cm and $\lambda = 24.5$ cm, corresponding to the two edges of the Arecibo multi-beam bandpass, 1225–1525 MHz. In the angular region bracketed by “o” the spectral index is positive. The apparent spectral index $\beta > 7$ in the sky region in the thin annuli bounded by the radii: $[1.469, 1.483]\theta_0$.

4. THE AMAZING SPECTRAL INDEX

There are three possible ways by which a source with an intrinsic spectral index of, say, $\alpha \approx -1$ (such a spectral index is routinely seen in high brightness sources), can manifest to the observer as a source with a large positive spectral index: (1) due to chromatic response of the side-lobe(s) of a telescope (2) due to multi-path propagation in the ISM which could result in chromatic scintillation and (3) due to free-free absorption caused by an intervening nebula. Below we discuss these three options.

4.1. Induced by the Telescope?

Spitler and co-authors attribute the amazing spectral index to the chromatic response of the side lobes of radio telescopes. Recall that the beam response of a diffraction limited telescope is a function of θ/θ_D where θ is the angle between the principal axis and the line-of-sight to the source and $\theta_D = \lambda/\mathcal{D}$ is the diffraction angular scale. Owing to this wavelength (frequency) dependence on the response, as can be seen from Figure 2, there are regions in the sky where the first side-lobe of a higher frequency band will have a larger response relative to the first side-lobe of the lower frequency. However, these regions are so small that the right phrase is “apparent large spectral index is manifested in small slivers of the sky”.

The correct way to evaluate the fraction of sources that would acquire a positive spectral index is to evaluate the volume probed by each elementary solid angle, $d\Omega$, of the Arecibo multi-beam and then take the ratio of the sum of the volumes of those elementary solid angles for which the response induces a large positive spectral index to that of the total volume probed. The elementary volume, $dV \propto d\Omega R^3$ where R is the distance to which a source with the minimum SNR can be detected. The conversion between S and R requires a knowledge of the FRB pop-

ulation. Let the daily all-sky rate of FRBs with fluence greater than a given value be represented by the following model: $N(> \mathcal{F}) \propto \mathcal{F}^q$. For a non-evolving source population and Euclidian geometry, $q = -3/2$. On axis, the telescope gain is large and the minimum SNR source has large R and a correspondingly large dV . For sources which are detected via side-lobes, the antenna gain is small and this leads to a correspondingly smaller R and thence smaller dV (see Figure 3 for a graphical demonstration of this point). Sources which exhibit an apparent spectral index > 7 (owing to chromatic beam response; see Figure 2) occupy a tiny fraction of the total volume (Figure 3).

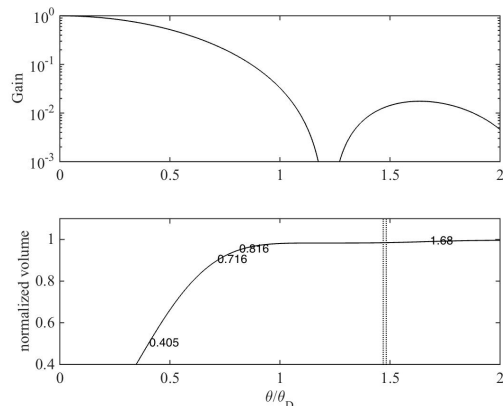


FIG. 3.— For the circular clear aperture discussed in Figure 2 the beam response (top) and the cumulative normalized volume, V , as a function of θ/θ_D . The angular radius at which [50%, 90%, 95%, 99%] of the cumulative volume (normalized to unity for large angular radius) is displayed along the curve (from left to right). Note most of the sources will be found inside of the first null. The two vertical lines mark the angular region in which the spectral index exceeds 7 (see caption to Figure 2). The fractional volume for $\beta > 7$ is 4×10^{-3} .

For a source population with $q = -3/2$, using the accepted Arecibo multi-beam response model, we find the following fractions: 0.4% and 0.1% for $\beta = [7, 11]$; see Figure 4 for graphical summary. These are upper limits since for $7 < \beta < 11$ the band-integrated fluence for a side-lobe detection is further reduced due to chromatic beam response (the reduction is relative to that of an FRB which is detected in the main beam). The additional factor of reduction is about 2 (see §A for explanation.) The resulting additional suppression in the volume is then $2^{-3/2} \approx 0.36$. Thus, the odds of detecting a normal FRB in a side-lobe (so that a large spectral index, $\beta \geq 7$ is obtained) is 1 out of 700. These odds are low enough that we consider it is not likely that chromatic response from the telescope resulted in the observed large spectral index.¹⁴

4.2. Induced by Multi-path Propagation?

Turbulence (density variations) in the ISM result in multiple rays from the source reaching the observer. This phenomenon is well known to pulsar astronomers

¹⁴ A simple way to test this idea is to determine the fraction of pulsars or RRATs with apparently large β (relative to the entire sample) discovered by Arecibo multi-beam survey.

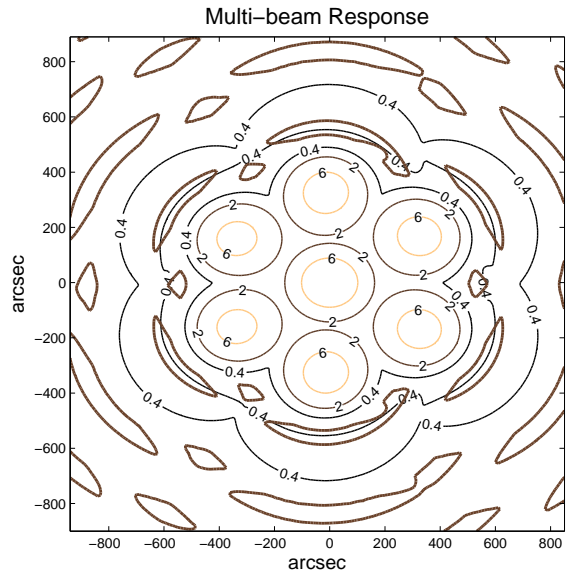


FIG. 4.— The gain of the Arecibo 7-beam receiver as a function of zenith distance and azimuth (both in arc seconds). Only three contours of the gain are shown: 0.4 K/Jy, 2 K/Jy and 6 K/Jy. The regions of the sky where spectral indices of 7 (or larger), assuming an input spectrum with spectral index of zero, can be produced are enclosed by dark lines. The central beam is “beam 0” and the six outer beams are beams 1 through 6 (clockwise). Since the telescope is alt-az the sky orientation of the beams will depend on the hour angle (and local sidereal time). The beam model used here was provided by L. Spitler.

as “interstellar scattering and scintillation” (ISS). There are two simple consequences: angular broadening of the source and the temporal broadening of a narrow pulse of radiation (“scattering tails”). If the turbulence is strong then ISS can lead to frequency dependent scintillation.

According to Bhat *et al.* (2004), τ_d , the broadening timescale at 1.4 GHz for a DM of $188 \text{ cm}^{-3} \text{ pc}$ ranges from $2.7 \mu\text{s}$ to 2.7 ms . The de-correlation bandwidth is $\Delta\nu_d = (2\pi\tau_d)^{-1}$ and is no larger than 6 MHz – far too small to account for the the doubling of frequency over more than 100 MHz. It is quite reasonable for us to conclude that FRB 121102 cannot be an extra-galactic source which suffered multi-path propagation and as a result exhibited an apparent β of 7 to 11.

4.3. Induced by Intervening Absorber?

In the decimetric band the primary absorption mechanism is free-free absorption. The free-free optical depth, τ_{ff} , is proportional to $\int \phi n_e^2 dl$ where n_e is the density of electrons, ϕ is the filling factor of clumps of electrons and the integral is along the line-of-sight. The constant of proportionality is temperature dependent. There are two possible temperature regimes: a low temperature regime (corresponding to a photo-ionized nebulae) and a high temperature regime (corresponding to stellar corona). Loeb, Shvartzvald & Maoz (2014) have proposed a model in which FRBs arise in the corona of stars. The combination of high temperature and large radius that is needed for this model will result in violent outflows and strong X-ray emission (see §7 of K14). The expected X-ray emission scales as DM^6 . With FRBs now

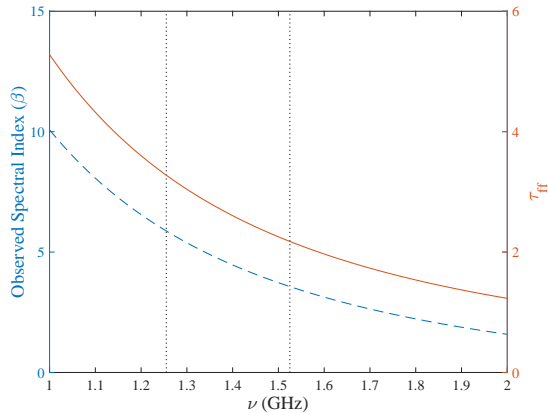


FIG. 5.— (Right y-axis; solid line): The free-free optical depth as a function of frequency, $\tau_{\text{ff}} = \tau(\nu_0)(\nu/\nu_0)^{-2.1}$ with $\tau(\nu_0)$ set to 2.5. (Left y-axis; dashed line): The observed spectral index, $\beta(\nu)$ for an input power law spectrum with $\alpha = -1$; see Equation 4 for the definition of β . The dotted vertical lines indicate the edges of the Arecibo multi-beam bandpass.

being reported with DM approaching $2,000 \text{ cm}^{-3} \text{ pc}$ the model is severely challenged, on observational grounds. So we will not discuss it anymore in this paper. Here, we consider the low temperature option – an intervening Galactic photo-ionized nebula.

The temperature of photo-ionized nebulae lie in a narrow range around $T_e \sim 8,000 \text{ K}$. In this frequency range the free-free absorption depth is given by

$$\tau_{\text{ff}}(\nu) = 4.4 \times 10^{-7} \text{EM} \left(\frac{T_e}{8,000 \text{ K}} \right)^{-1.35} \left(\frac{\nu}{1 \text{ GHz}} \right)^{-2.1} \quad (3)$$

where $\text{EM} = \int n_e^2 dl$ is the “emission measure”; the unit is $\text{cm}^{-6} \text{ pc}$ (Lang 1980, p. 47)

The spectrum of an FRB with foreground free-free absorption is then $f(\nu) = S(\nu) \exp(-\tau_{\text{ff}})$ where $S(\nu)$ is the intrinsic spectrum. At each frequency one can define an apparent spectral index

$$\begin{aligned} \beta(\nu) &\equiv \frac{d \log f(\nu)}{d \log \nu} \\ &= \alpha - \tau_0 \left(\frac{\nu}{\nu_0} \right)^{-2.1} \end{aligned} \quad (4)$$

where the input spectrum is a power law, $S(\nu) \propto \nu^\alpha$. In Figure 5 we plot $\beta(\nu)$ across the Arecibo bandpass. We choose the normalization, $\tau(\nu_0) = 2.5$ so that the mean spectral index over the Arecibo bandpass is 5. We made this conservative choice¹⁵ since the apparent spectral index is known to be covariant with the peak flux (S14).

With the chosen normalization, using Equation 3 we find $\text{EM} \approx 1.2 \times 10^7 \text{ cm}^{-2} \text{ pc}$. The resulting absorbed broad-band spectrum is displayed in Figure 6. Note that even at the high frequency edge the input flux is absorbed by nearly an order of magnitude.

4.4. Summing up: Spectral Index

¹⁵ As can be seen from Equation 4, over the range expected for α of say 1 to -2 , the inferred value of τ_0 is quite robust.

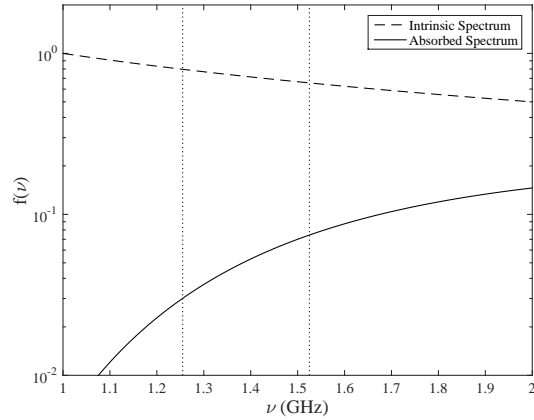


FIG. 6.— The broad-band input spectrum (dashed line) and the output spectrum after undergoing free-free absorption of an FRB with intrinsic spectral index of $\alpha = -1$. The free-free optical depth is $\tau(\nu_0) = 2.5$. The thin dotted vertical lines mark the lower and upper frequency limits of the Arecibo multi-beam system

In this section we considered three possible mechanisms to transmute an intrinsic spectral index of $\alpha = -1$ to an apparent spectral index between 7 and 11. We reject the proposal that Galactic interstellar medium could, as a result of ISS, produce such a large spectral index. We find the odds of FRB 121102 to be in a side-lobe to be 1 in 700 (relative to an FRB found in the main beam) and thus strongly disfavor chromatic side-lobe response as being responsible for the large observed spectral index. By process of elimination we arrive at the hypothesis that the positive spectral index is due to absorption by an intervening nebula. There are two possibilities for the location of the intervening nebula: Galactic or extragalactic. In the next section we investigate the properties of the putative Galactic nebula.

5. THE INTERVENING NEBULA (GALACTIC)

In this section, accepting the framework in which FRB 121102 suffered from significant free-free absorption, we now attempt to infer the physical properties of the intervening free-free absorbing nebula. In part this hypothesis is motivated by the fact that FRB 121102 is located at low Galactic latitude, admittedly in the Galactic anti-center.

The primary parameters for the intervening Galactic nebula model are the following: L , the thickness of the nebula (the length along the line-of-sight); D , the diameter in the plane of the sky; and d , the distance from us to the source. Our challenge is to see if observations can constrain these parameters (and better still if the nebula is actually detected in archival data or could be detectable by near-future observations). We make the reasonable assumption that L is comparable to D (spherical approximation). Sheets are not uncommon structures in the ISM and so $D \gg L$. However, on purely probabilistic ground, $D \ll L$ is not likely.

The two constraints for the putative nebula are the free-free optical depth ($\tau_{\text{ff}} \propto \text{EM}$; see Equation 3) induced by the nebula, and the dispersion measure (DM') arising inside the nebula. For the former we have already determined $\text{EM} \approx 1.2 \times 10^7 \text{ cm}^{-6} \text{ pc}$ (§4.3). There is little reason to believe that there will be significant

contribution to EM by the diffuse Galactic ISM. The inferred DM of $557 \text{ cm}^{-3} \text{ pc}$ is due to (i) Galactic contribution and (2) contribution from the nebula. We assign $DM' = 400 \text{ cm}^{-3} \text{ pc}$.

Both DM' and EM are line integrals of moments of electron distribution along the path to the source. We derive two fundamental parameters of the nebula:

$$n_e = \frac{EM}{DM'} = 3 \times 10^4 \text{ cm}^{-3}, \quad (5)$$

$$\phi L = \frac{DM'^2}{EM} = 0.013 \text{ pc}. \quad (6)$$

Going forward we will set $\phi = 1$. The electron density is low enough that the plasma frequency, $\nu_p = \sqrt{n_e e^2 / (\pi m_e)} = 1.6 \text{ MHz}$, is well below the observing frequency. The mass in the nebula (assuming only Hydrogen) is $\approx 10^{-3} (D/L)^2 M_\odot$.

Since the nebula is optically thick in the band under consideration ($\tau \approx 2.5$; see §4.3), the surface brightness is simply given by the Rayleigh Jeans formula:

$$I(1.4 \text{ GHz}) = 12(T_e/8,000 \text{ K}) \text{ mJy arcsec}^{-2}. \quad (7)$$

In the $H\alpha$ line the surface brightness is related to EM as follows (see K14)

$$I(H\alpha) = 1.09 \times 10^{-7} EM \text{ erg cm}^{-2} \text{ s}^{-1} \text{ sr}^{-1}. \quad (8)$$

Given that $EM \approx 1.2 \times 10^7 \text{ cm}^{-6} \text{ pc}$ (§4.3) we find the expected surface brightness is

$$I(H\alpha) = 3.1 \times 10^{-11} \text{ erg cm}^{-2} \text{ arcsec}^{-2}. \quad (9)$$

It is illustrative to convert this intensity to photon units: $I(H\alpha) \approx 10.1 \text{ photon cm}^{-2} \text{ s}^{-1} \text{ arcsec}^{-2}$. In contrast, the night sky (new moon) has a brightness of $21 \text{ mag arcsec}^{-2}$ in the R-band. This corresponds to a photon surface brightness of $4 \times 10^{-3} \text{ photon cm}^{-2} \text{ s}^{-1}$.

The angular size of the nebula is

$$\theta_N = 2.75'' (D/L) d_{\text{kpc}}^{-1} \quad (10)$$

where d_{kpc} is the distance to the nebula in pc. Integrating $I(H\alpha)$ over the angular extent of the nebula yields an $H\alpha$ flux density of

$$f(H\alpha) = I(H\alpha) (\pi/4) \theta_N^2 \\ = 1.83 \times 10^{-10} (D/L)^2 d_{\text{kpc}}^{-2} \text{ erg cm}^{-2} \text{ s}^{-1}. \quad (11)$$

In the 21-cm band, by construction, the nebula is optically thick and so the Rayleigh-Jeans formula (Equation 7) provides the expected surface brightness. The flux density is then

$$S = \frac{\pi}{4} \theta_N^2 I(1.4 \text{ GHz}) \\ = 71 (T_e/8,000 \text{ K}) (D/L)^2 d_{\text{kpc}}^{-2} \text{ mJy} \quad (12)$$

The number of recombinations per second is

$$\dot{N}_R \approx \frac{\pi}{4} \alpha_B D^2 L n_e^2 = 0.54 \times 10^{46} (D/L)^2 \text{ s}^{-1}. \quad (13)$$

Here, $\alpha_B = 1.1 \times 10^{-13} (T_e/8,000 \text{ K})^{-0.89} \text{ cm}^3 \text{ s}^{-1}$ is the Case B recombination (Osterbrock & Ferland 2006). If the nebula was photo-ionized then the corresponding *minimum* ionizing (UV) luminosity is

$$L_{UV} > 4 \times 10^{35} (D/L)^2 \text{ erg s}^{-1}. \quad (14)$$

TABLE 1
NVSS SOURCES IN THE FIELD OF FRB 121102

Name	RA	Dec	$\Delta\theta$	Flux (mJy)
AFRB	05 32 9.6	+33 05 14	0''	–
VLA1	05 32 09.7	+33 04 05	69''	3.2 ± 0.4
VLA2	05 31 53.8	+33 10 15	308''	4.6 ± 0.5

NOTE. — The nominal position of FRB 121102 (“AFRB”). The search radius was 413 arc seconds. The two sources, VLA1 and VLA2 are from the NRAO VLA Sky Survey (NVSS). $\Delta\theta$ is the radial offsets of the VLA sources from AFRB.

If a similar continuum flux is available at say 2500 \AA and 4500 \AA then the AB magnitude will be $13.7 + 5 \log(d_{\text{kpc}})$ and $13.0 + 5 \log(d_{\text{kpc}})$ mag, respectively,

5.1. Search for Counterpart

Next, we conducted a search of relevant archival data sets for the counterpart of the putative nebula. Specifically we restricted the search to a circular region of radius 413 arc seconds and centered on beam 4. The radius is large enough to include the side-lobe response to 0.4 K/Jy (which incidentally is approximately equal the on-axis gain of the Parkes telescope; see Figure 4). Below we describe the result of this search.

5.1.1. Decimetric Band

The fruits of our search of the VLA Sky Survey (Condon *et al.* 1998) – a survey which mapped the entire Northern Sky in the 21-cm band – can be found in Table 1. The two sources are nominally noted to be unresolved in the NVSS catalog and do not correspond to any source in the IPHAS catalog (see 5.1.2). Likely they are background radio sources. Nonetheless, comparing Equation 12 with $D \approx L$ to the flux of the two sources we find $d_{\text{kpc}} > 4.2 \text{ kpc}$.

5.1.2. IPHAS

Using the Isaac Newton Telescope and a mosaic of CCDs the Northern Galactic plane was imaged – the Isaac Newton Telescope Photometric Halpha Survey or IPHAS (Drew *et al.* 2005). The survey was undertaken in three bands: r' , i' and a custom narrow-band filter centered on $H\alpha$ at zero velocity (6563 \AA) and a full-width-at-half-maximum (FWHM) bandpass of 95 \AA (hereafter, we will refer to this band as ha). All the magnitudes are referenced to the Vega system and the assumed zero point(s) are given in Appendix D.

We inspected the ha image carefully and found no evidence of an extended nebula, as would be expected for a source located at say 1 kpc (cf. see Equation 10). This motivates us to consider a source at, say, 10 kpc. In this case, the nebula will appear point like.

Combining Equation 11 and Equation D2 we obtain the following equation:

$$ha = 7.8 + 5 \log(d_{\text{kpc}}) \quad (15)$$

Thus, even for a source at 20 kpc (a plausible distance that places the source at the known edge of the Galaxy) we would expect to see bright $H\alpha$ source, $ha \approx 14.3$. To

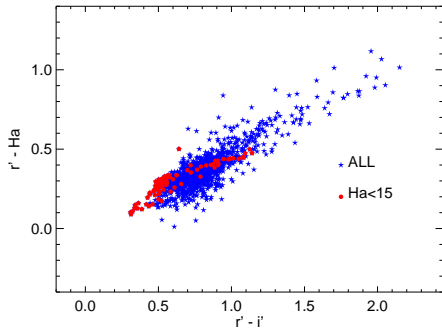


FIG. 7.— The $r' - H\alpha$ (ha) and $r' - i'$ color-color diagram for the IPHAS sources in the error circle of FRB 121102. We examined all objects with $ha < 15.0$ (shown as red filled circles). They are consistent with being ordinary stars.

be conservative, we examined all objects with ha brighter than $ha = 15$ (red filled circles in Figure 7).

This figure is identical to Figure 1 in Witham *et al.* (2006), in which the authors use IPHAS photometry to identify $H\alpha$ emitting sources. Their figure shows that normal stars with magnitudes brighter than $r' = 16$ occupy a small region along the line delineated by the majority of objects, while outliers above this cloud are candidate $H\alpha$ emitters. The scatter in the stellar distribution is due to variations in the extinction along the line-of-sight to stars of varying distances. Figure 7 shows only one candidate outlier above the distribution shown by the red filled circles, which is TYC 2407-679-1, an A star ($B - V \cong 0.3$ mag).

We also searched the catalog for objects that were detected in ha , but not in the other filters and only two objects met this criterion, J053232.67+330840.0 at $ha = 19.3$, and J053211.51+330419.8 at $ha = 19.4$. Both of these objects are too faint to be the nebular counterpart that produced the FRB.

5.1.3. The PTF $H\alpha$ Survey

The primary goal of the Palomar Transient Factory (Law *et al.* 2009; Rau *et al.* 2009) is a systematic study of the transient optical sky. To this end the dark and gray time is used to undertake a number of “experiments” in g and R bands. However, during three nights around full moon, the PTF collaboration has been undertaking a Census of the Local Universe (CLU) survey to complete our catalog of nearby galaxies. CLU deploys four contiguous narrow-band filters to search for extended, $H\alpha$ emitters across 3π of the Northern sky out to a distance of 200 Mpc (Kasliwal 2011). CLU assists the discovery of local Universe transients by providing a host galaxy redshift which is a severe filter to channel follow-up. For example, CLU helps pinpoint electromagnetic counterparts to gravitational waves in two ways (i) for wide-angle optical searches, CLU promptly reduces false positives by two orders of magnitude (Kasliwal & Nissanke 2014; Nissanke, Kasliwal & Georgieva 2013) (ii) for narrow-field X-ray/infrared searches, CLU helps determine the top pointings (Gehrels *et al.* 2015).

For the purpose of the discussion here only two bands

are relevant: centered on the rest frame $H\alpha$ at 656 nm (“ $H\alpha$ -on”) and the other on 663 nm (“ $H\alpha$ -off”). PTF obtained 14 images in each one of the filters. We co-added the images taken in each filter using *SWarp* (Bertin 2010). The images are presented in Figure 8.

The basic data reduction of PTF data is described in Laher *et al.* (2014). The PTF $H\alpha$ survey is still being calibrated. We undertook the following *rough* calibration. Following the prescription in Ofek *et al.* (2012) we calibrated the image using the Tycho 2 star at $RA=83^{\circ}.07877$ $Dec=+33^{\circ}.192993$. Fitting its B_T, V_T, J, H, K magnitudes with the Pickles (1998) main sequence stars spectral templates, we found a best fit with a spectral class F5V. Using its spectral template we calculate the star $H\alpha$ flux from synthetic photometry of an F5V template. We found the star AB magnitudes are 11.87 and 11.80 in $H\alpha$ -on and $H\alpha$ -off bands, respectively. The Zero Point (ZP) for the $H\alpha$ image is 24.05 AB mag.

A number of point sources exhibit $H\alpha$ in emission. The point sources range from 17.3 AB mag to 19.3 AB mag (the detection limit). In an effort to search for diffuse emission we smoothed the difference image. The brightest sources in the nebosity in the image are about 20 AB mag per 10×10 arcsec² (corresponding to 0.036 mJy). In summary both the IPHAS and PTF analysis shows that any putative intervening nebula is beyond 20 kpc – beyond the edge of the Galaxy in this direction.

5.2. Summing Up: Galactic Nebula

In summary, we searched for a putative Galactic compact nebula which could produce the necessary free-free absorption. We found no evidence in the radio (free-free continuum) nor $H\alpha$ (recombination radiation). We can rule out that the necessary nebula does not exist, at least within the galaxy (say a distance of up to 20 kpc which would certainly mark the edge of the Galaxy in this direction). So we conclude that were FRB 121102 to be extragalactic then the intervening nebula must be located in the host galaxy of FRB 121102. The inferred density of the intervening nebula (see Equation 5) is clearly atypical for diffuse ISM. FRB 121102 must thus be associated with a region of rich ISM (and thence high star-formation).

On a separate but important issue we note that the failure to find a compact nebula also rules out a purely Galactic explanation for FRB 121102, namely, a Rotating Radio Transient (RRAT) with a conveniently arranged intervening nebula (cf. the radio burst discussed by Keane *et al.* 2012).

6. THE LOCALE OF FRBS

Here, we gather our thoughts on the origin of FRBs. By treating the Parkes and the Arecibo FRBs as a single class, we can state with some confidence that FRBs must be located beyond 100 km. This then opens up three reasonable locales: the ionosphere, the Galaxy and other galaxies. In the ionosphere model, a ball of charged particles somehow produce millisecond bursts in the decimetric band and whose emission follows a $t_a \propto \nu^m$ with $m = -2$ to good precision. Furthermore, in some cases the pulse has to be broadened by milliseconds (ms). The usual explanation for “scattering” tails is multi-path propagation. The scattering time scale of a radio pulse

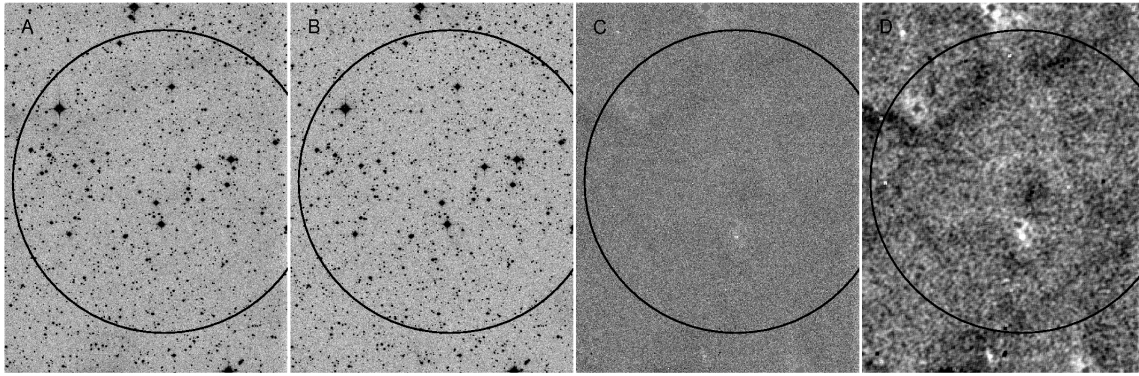


FIG. 8.— From left to right. [A] Co-addition of 14 PTF H α (656 nm) images. [B] Co-addition of 14 PTF H α -off (663 nm) images. [C] The on-off subtracted image using a custom image subtraction algorithm (Zackay, Ofek & Gal-Yam, in prep). [D] The subtracted image smoothed by a square of side 10'' top hat filter to identify faint-extended features. The grayscale is inverted. In particular, for panel C and D, positive signal is black. The white patches are artifacts due to wings of bright stars.

is given by

$$\tau_d = \frac{1}{2c} \theta^2 \frac{D_l D_s}{D_{ls}}, \quad (16)$$

where D_l , D_s and D_{ls} are the distances to the scattering screen, the source and scattering screen to the source, respectively. Due to the scattering the source angular size will be amplified to θ . An important point is that if the source is nearby, in order to get a scattering over 1 ms, the angular size of the source will have to be larger than the beam size, and hence it will be detected in multiple beams. Therefore, we can use this to set a lower limit on the distance to FRBs. Setting $\tau_d = 1$ ms, and $\theta < 11$ arcmin, we find that $D_s \gtrsim 10^{-3}$ AU which far exceeds the size of the ionosphere. So, as with the measured DM, we need to find an alternative explanation for the scattering tails.

We have thoroughly investigated a possible Galactic origin (in which most of the inferred intervening electrons arise in a Galactic nebula) for FRB 010724 (K14) and here we have undertaken a similar investigation for FRB 121102. In both cases, we did not find any evidence to support a Galactic origin.

We thus find ourselves between two exotic possibilities: (i) an entirely unknown ionospheric phenomenon with particularly exotic (a more accurate word is “tailored”) properties or (ii) an extra-galactic phenomenon in which the frequency dependent arrival time, scattering tails and occasional free-free absorption can be readily accounted. The primary challenge for the extra-galactic model is that the FRB pulses are as brilliant as those of pulsars but last *six orders of magnitude* longer or equivalently arise in regions which are six orders of magnitude larger than those of pulsars. The energetics in the radio alone is staggering. Two decades ago astronomers were in a similar quandary in regard to the origin of GRBs: an increasingly exotic local model and a simpler extra-galactic model but with extra-ordinarily large power and energy demands. We have exhausted all reasonable Galactic options and being forced to consider “designer” models with increasingly strident demands for the terrestrial option. Guided by the history of our field, we are driven to the extra-galactic model. The rest of the paper is an exploration of the extra-galactic model.

7. AN EXTRA-GALACTIC ORIGIN

In the extra-galactic model for FRB 121102, the dispersion measure in excess of the Galactic contribution is about $370 \text{ cm}^{-3} \text{ pc}$. This is due to contribution from electrons in the intergalactic medium, electrons in the diffuse interstellar medium (ISM) and from electrons in the dense nebula close to the FRB source. The reason we are forced to invoke a dense nebula is that neither the IGM nor the host diffuse ISM (along most lines of sight) would have an emission measure so high as to produce $\tau(\nu_0) \approx 2.5$.

This intervening EM-inducing nebula will also contribute to the dispersion measure. Lacking any additional information, we apportion the excess dispersion measure (above) about equally to the IGM (say, $\text{DM}_{\text{IGM}} \approx 170 \text{ cm}^{-3} \text{ pc}$) and to the dense nebula ($\text{DM}'' \approx 200 \text{ cm}^{-3} \text{ pc}$).

In the extra-galactic framework, the distance to an FRB, d_{IGM} , is inferred from DM_{IGM} and the use of an accepted model for the mean density of the IGM plasma as a function of redshift (e.g. Ioka 2003; Zheng *et al.* 2014). With this assignment the inferred redshift to the host galaxy is reduced to $z \approx 0.19$. The density and the width of the intervening plasma, relative to that discussed in §5, is a factor of two higher and a factor of four lower respectively (see Equations 5 and 6). Thus, $n_e = 6 \times 10^4 \text{ cm}^{-3}$ and $L = 3.3 \times 10^{-3} \text{ pc}$.

In the absence of free-free absorption the peak flux of FRB 121102 is about ten times higher than that observed (see Figure 6). FRB 121102, had it not been for the absorption by the compact nebula, would have been as bright as the typical Parkes FRB.

7.1. Volumetric Rate of FRBs

At the present time, FRBs are localized to fractions of square degrees and this localization is simply not good enough to securely identify FRBs with other galaxies. Let \mathcal{R} be the daily all-sky rate of detected FRBs. According to Keane & Petroff (2015),

$$\mathcal{R}(\mathcal{F} \geq 2 \text{ Jy ms}) \approx 2500 \text{ day}^{-1}. \quad (17)$$

With the distances inferred from DM_{IGM} (§7), the inferred the volumetric rate of FRBs is

$$\Phi_{\text{FRB}}(\mathcal{F} > 2 \text{ Jy ms}) = 6 \times 10^3 \text{ Gpc}^{-3} \text{ yr}^{-1}; \quad (18)$$

see K14 for details. Any proposed extra-galactic model for FRBs must demonstrate that a radio signal can propagate from the explosive site without significant absorption. Separately, the same model must account for the FRB volumetric rate.

Following K14, on physical grounds we reject both major families of supernovae (core-collapse, Type Ia) and long duration gamma-ray bursts (both low and high luminosity). The volumetric rate of short-hard bursts is clearly insufficient to account for Φ_{FRB} . The *blitzar* model in which FRBs originate from massive NS collapsing into BHs was cleverly designed to avoid the problem of significant free-free absorption (Falcke & Rezzolla 2014). However, this model cannot be reconciled with the demographics of Galactic pulsars and also that of bright supernovae (K14). So we reject the blitzar model as well. In the next section we explore the model which avoids the key physical fatal flaw (local absorption) and the physical requirement of possessing sufficiently large volumetric rates.

8. GIANT FLARES AS CAUSING FRBS

There are three reasons why we find the model in which FRBs result from Giant Flares from SGRs. First, as with pulsars there is very little absorbing matter in the immediate vicinity of SGRs. Thus, there is no impediment to the transmission of radio pulses. Next, the volumetric rate of giant flares is well matched to that of FRBs (see below). Finally, a physically plausible model in which giant flares from SGRs give rise to FRBs has been proposed (Lyubarsky 2014).

According to Ofek (2007) the volumetric rate of giant flares from SGRs is as follows:

$$\Phi_{GF}(\mathcal{E}_\gamma \lesssim \mathcal{E}_*) < 2.5 \times 10^4 \text{ Gpc}^{-3} \text{ yr}^{-1} \quad (19)$$

$$\Phi_{GF}(\mathcal{E}_\gamma \gtrsim \mathcal{E}_1) \approx 4 \times 10^5 (\tau_{GF}/25 \text{ yr})^{-1} \text{ Gpc}^3 \text{ yr}^{-1} \quad (20)$$

where $\mathcal{E}_* = 3.6 \times 10^{46}$ erg, $\mathcal{E}_1 = 3 \times 10^{44}$ erg and τ_{GF} is the mean time between giant flares; $\tau_{GF} > 30$ yr at the 95% confidence level (Ofek 2007). We will refer to flares with $\mathcal{E} \approx \mathcal{E}_*$ as “hyper-giant” flares (HGF) and those with energy comparable to \mathcal{E}_1 as giant flares.

The isotropic energy release of a 1 Jy FRB with $\alpha = -1$ and lasting 1 ms is $10^{39} d_{\text{Gpc}}^2$ erg; here d_{Gpc} is the distance to the FRB in units of Gpc. The unknown and key issue is the efficiency, η , with which the giant flare energy (primarily in γ -rays) can be converted to a brilliant radio pulse. If η can be as large as 10^{-5} then there is comfortable margin between the volumetric rate of detected FRBs (Equation 18) and that of the giant flares from SGRs (Equation 20). If η is much smaller, say 10^{-7} then the relevant SGR rate is that of Hyper-giant flares (Equation 19) and the margin between the FRB rate and the HGF rate is less than a factor of four.

8.1. A Young Magnetar Model

In our Galaxy giant flares have been seen from two young magnetars: SGR 1806–20 (age, 650 ± 300 yr) and SGR 1900+14, age $(6 \pm 1.8) \times 10^3$ yr (Tendulkar, Cameron

& Kulkarni 2013). Both these magnetars are associated with star clusters (see Tendulkar, Cameron & Kulkarni (2013) for summary). A dense ISM is seen in the vicinity of SGR 1806–20 and a near-IR dust ring or shell has been noted around SGR 1900+14 (Wachter *et al.* 2008). Motivated by this basic observation we propose that FRBs result from *young* magnetars. A natural consequence of this model is the presence of a rich ISM on scales of a parsec (as in SGR 1900+14) to a size set by region of intense star formation (tens to hundreds of parsecs).

The young magnetar model can readily explain the presence of a dense ISM, as inferred for the case of FRB 121102. Most FRBs exhibit an exponential decay with timescales, $\tau_d \sim 1$ ms. This “tail” is attributed to multi-path propagation induced by turbulent structures. The young magnetar hypothesis naturally accounts for such scattering tails.

Star-forming regions, specifically HII regions and supernovae shells are known for having turbulent structures. The angular broadening, θ_s , at the fiducial frequency, expected from the inferred turbulence (“scattering measure”) in prominent Galactic HII regions (e.g. NGC 6334; Cygnus star forming region; Galactic Center) is $\theta_s \sim 0.1$ – $1''$ (see §11 of K14). Angular broadening leads to multi-path propagation with an exponential timescale of

$$\tau_d = \frac{D_s}{2c} \theta_s^2 \quad (21)$$

where D_s is the distance from the FRB (magnetar) to the turbulent medium. Thus, a turbulent medium at, say, $D_s \sim 10$ – 100 pc would easily account for the scattering tails.

8.2. The Orion Star-forming Region

In order to concretely understand the ramifications of the young magnetar model, some familiarity of the locales (in this hypothesis) would be useful. To this end, consider the Orion nebula. It is not a particularly rich cluster (relative to those of SGR 1900+14 and SGR 1806–20). However, it is one of the best studied objects in modern astronomy.

The diameter of Orion nebula is 8 pc. The peak optical depth at 1.4 GHz is 0.055 and the corresponding EM is $2.5 \times 10^5 \text{ cm}^{-3} \text{ pc}$ (Felli *et al.* 1993). Thus, the mean density of Orion is 177 cm^{-3} and the corresponding maximum DM would be $1416 \text{ cm}^{-3} \text{ pc}$. However, the structure of Orion nebula is, as is the case with other star forming regions, complex. On one side, the newly born cluster of hot stars are irradiating and ionizing the parental molecular cloud and this in turn is likely to initiate new star formation inside the cloud. On the opposite side the ionized gas is flowing away from the star cluster.

The ionization structures of the Orion nebula are summarized in Table 2. The magnetic field in Orion is comparable to the thermal pressure (Ferland 2001) or about 0.4 mG. The resulting EM, DM and RM are summarized in Table 2. The point of this table is to expose the reader to the complexities of real star clusters (and their rich ISM) and, in particular, to the potentially large contribution to DM, EM and even rotation measure (RM; see §9 for definition of RM).

8.3. A Nuclear Magnetar Model

TABLE 2
PHYSICAL PARAMETERS FOR THE ORION NEBULA

Zone	n_e cm^{-3}	l pc	DM $\text{cm}^{-3} \text{pc}$	EM $\text{cm}^{-6} \text{pc}$	RM m^{-2}
PDR	10^5	?	–	–	–
IF	> 6000	10^{-4}	> 0.6	$> 3.6 \times 10^3$	$> 1.9 \times 10^2$
Low Ion.	7000	2×10^{-3}	14	9.8×10^4	4.5×10^3
Med Ion.	4000	0.06	240	9.6×10^5	7.7×10^4

NOTE. — PDR: Photodissociation region. IF: Ionization Front. The temperature and densities are from O’dell (2001).

Pen & Connor (2015), motivated by the discovery of SGR J1745–2900, have proposed that FRBs arise from magnetars located in the centers of galaxies (hereafter, “nuclear magnetars”). The DM and RM of this object is, as expected, extra-ordinary: $1650 \text{ cm}^{-3} \text{ pc}$ and -67000 m^{-2} , respectively (Shannon & Johnston 2013). If such a large contribution is accepted to the measured DM then a consequence is a vast reduction¹⁶ in the inferred distances to FRBs.

We are puzzled by the hypothesis of nuclear magnetars. There is nothing special about SGR J1745–2900 other than its nuclear location. There are several magnetars similar to SGR J1745–2900, a middle-aged and relatively quiet object, in other locations of the Galaxy. Any nuclear magnetar model must state what makes nuclear magnetars special enough to become the sole source of FRBs. Next, the model is silent on a key observational demand – is the population of active nuclear magnetars able to account for the observed sky rate of FRBs?

8.4. Young Pulsars

Connor, Sievers & Pen (2015) have proposed a model in which young extra-galactic pulsars, still within their supernova remnants, produce bright radio pulses which we see as FRBs. The supernova remnants contribute significantly to the DM. The typical distance to FRBs, in this framework, is 200 Mpc. In the introduction to §6 we noted the physical limitation of this model: the giant pulses of pulsars are extremely short (nanosecond corresponding to length scales of a meter; Hankins *et al.* 2003). In order to produce FRBs we need coherently emitting regions which are a few light milliseconds wide (10^{11} cm) – far in excess of the magnetosphere of young pulsars. Regardless of this theoretical issue the model is testable. The error circles of FRBs should contain nearby ($< 200 \text{ Mpc}$) galaxies.

8.5. Summing up

In summary, the young magnetar model can account for the impressive volumetric rate of FRBs, the energetics and also neatly explain the circumstantial clues: scattering tails that are seen in most FRBs and the occasional FRB with strong free-free absorption.

We make the following parenthetical remark. We do not know what specific attribute of magnetars leads to the phenomenon of giant flares. Above we have discussed the only two known Galactic SGRs which have emitted hyper-giant flares. Both SGRs are associated

with star clusters. The hyper-giant flare of 5 March 1979 came from SGR 0525–66. This source is associated with a rich star-forming region in the Large Magellanic Cloud (Klose *et al.* 2004). The nominal characteristic age of SGR 0525–66 is 3.4 kyr (Olausen & Kaspi 2014). There are 14 magnetars (SGRs and AXPs) whose characteristic age is less than 10 kyr (see Olausen & Kaspi 2014). Two magnetars, 1E1547.0–5048 CXOU J171405.7–38103, have characteristic ages less than 1 kyr. Some magnetars are found close to the center of their supernova remnant. So while we do not know what makes only some magnetars emit giant flares we do know that almost all of them lie in ISM rich regions.

Continuing this parenthetical remark we note that Maoz *et al.* (2015) claim that two FRBs but with different DMs came from the same region in the sky. We have no independent assessment of this claim but note that it is entirely possible that a single galaxy, particularly one which is undergoing vigorous star-formation, to be capable of hosting two FRBs within a few years. The differing DMs could be due to differing contributions from the local star-forming regions in which the magnetars are located. After all, the Milky Way (including the Magellanic Clouds), a system with a modest star-formation rate of only $\approx 1 M_{\odot} \text{ yr}^{-1}$ (Robitaille & Whitney 2010), has hosted four hyper-giant flares in less than four decades. So it is quite reasonable that a galaxy like M51 which has star-formation rate three times that of our Galaxy could be three times more productive in giant flares relative to our Galaxy.

9. RAMIFICATIONS OF THE YOUNG MAGNETAR MODEL

In this section we explore the ramifications of the young magnetar model.

1. Young magnetars are found in star-forming regions of galaxies. Thus, the simplest consequence is that FRBs are not denizens of intergalactic space. If so, models involving non-stellar origin (e.g. exotic models involving super-conducting strings such as proposed by Vachaspati 2008) can be rejected.
2. Next, as noted in §7.1, the translation of \mathcal{R} to Φ_{FRB} is usually done assuming that the distance to the FRB is given by d_{IGM} . However, if we accept the central thesis of this paper – that FRBs are related to young SGRs, which in turn mark the richest star-forming regions in our Galaxy, then we also have to accept that a substantial contribution to the measured DM of an FRB could also arise in rich star-forming regions in the host galaxy (see discuss §8.1). Let $f = d/d_{\text{IGM}}$ where d is the true distance. It is likely that f is significantly smaller than unity.

The true FRB rate is

$$\Phi'_{\text{FRB}} = \langle f^{-3} \rangle \Phi_{\text{FRB}} \quad (22)$$

where $\langle \dots \rangle$ stands for the population average. FRBs which have small DM but exhibit scattering or absorption will contribute disproportionately to the true rate. Regardless, the true volumetric rate of FRBs is larger than had been hitherto discussed.

¹⁶ In this model, there would almost be no relation between the true distance, d and the DM.

Separately, the FRB all-sky rate (Equation 17) is based on FRBs with $\mathcal{F} > 2 \text{ Jy ms}$. Indeed, the rate of *detected* FRBs is nominally twice this rate (Champion *et al.* 2015). Thus, the volumetric rate of FRBs could be larger than that estimated by Equation 22. If these two factors lead to large corrections then it may well be that we need to invoke¹⁷ giant flares from SGRs to account for the increased volumetric rate of FRBs.

We cannot make f arbitrarily small. Let l_* be the “typical” distance to FRBs. The volumetric rate is the $\propto \mathcal{R}/l_*^3$. We equate this to the volumetric rate of Giant flares. With that we find $l_* \approx 0.8 \text{ Gpc}$. FRBs are still very impressive extra-galactic transients.

3. As can be gathered from the discussion leading to Equation 21, scattering tails require a highly turbulent medium. From basic considerations one expects significant EM to be associated with these turbulent regions (see §11 of K14). Clearly, the detected sample of FRBs, with the exception of FRB 121102, does not show strong free-free absorption at 1.4 GHz. However, the free-free optical depth scales as $\nu^{-2.1}$. Thus, a modest¹⁸ optical depth of $\tau_{\text{ff}} \approx 0.5$ at 1.4 GHz will result in significant suppression in the meter-wave band. This issue is worthy of further study by the developers of FRB searches with CHIME (400–800 MHz) and the refurbished Molonglo Telescope (843 MHz).
4. One event, FRB 140514, shows detectable circular polarization (Petroff *et al.* 2015). By analogy to the pulsar phenomena, we would expect FRBs to also exhibit linear polarization. A magnetized ISM will rotate the linear polarization vector by an angle

$$\theta(\lambda) = \text{RM} \lambda_m^2, \quad (23)$$

where λ_m is the wavelength in meters, and RM is the rotation measure, $0.81 \int n_e B dl$ with B , the magnetic field (along the line of sight) in units of μG and dl in units of pc; the units of RM is m^{-2} .

The young magnetar model predicts significant RM (hundreds m^{-2}) because of the increased magnetic field strength in HII regions (§8.2). In the case of FRB 121102, we expect a very large RM ($\sim 10^3 \text{ m}^{-2}$ or more) because the magnetic field in dense structures is expected to be significantly above the typical diffuse ISM value. Those FRBs which show scattering tails are expected to exhibit RMs larger than those which show no scattering tails.

Finally, for particularly bright FRBs, it may be possible to see the local H I and even some molecular species (OH) in absorption in the spectrum of the FRB. It would be worthwhile to design FRB hardware such that a high quality and reliably calibrated spectrum can be recovered from the raw data (post-discovery).

5. SGR flares are expected to be accompanied by highly relativistic ejecta. The isotropic γ -ray energy released in a hyper-giant flare is $3 \times 10^{46} \text{ erg}$. It is not unreasonable to assume that the ejecta has a kinetic energy comparable to the γ -ray energy release. In our model, in some cases, the ISM is close to the magnetar and so we expect the ejecta to slam into high density ISM. The resulting shock(s) can be expected to generate radio, X-ray and even very high energy photons that could last days to weeks. In contrast, the same explosion taking place in the average diffuse ISM will undergo a shock but on a longer timescale (e.g. type Ia supernovae).
6. A consequence of having a significant contribution to the observed DM from ISM structures in the vicinity of the FRB means that FRBs are noisy probes of the electron density and magnetic field in the IGM (cf. McQuinn 2014) and of cosmography (cf. Zhou *et al.* 2014; Gao, Li & Zhang 2014). Delicate tests of cosmography may prove to be challenging and frustrating (see also Pen & Connor (2015)). A possible way to minimize the outliers is to obtain the broad-band spectrum, from meter wave to centimeter wave, of FRBs. The broad-band spectrum will readily identify FRBs with large free-free absorption. However, this would require that facilities spanning a decade of frequency either be truly band-band or enjoy common view.

But all of this is speculation. A clear test (and vindication) of the SGR model is the detection of an FRB contemporaneous with a soft γ -ray burst detection.

We are grateful to Dr. Laura Spitler for providing us the beam response files. We thank the PTF collaboration and in particular M. Kasliwal and D. Cook for allowing us to showcase the PTF H α data ahead of a formal data release. We would like to thank Glenn Jones for asking us to consider Galactic ISS as a possible explanation for the large spectral index. SRK’s research, in part, is supported by a grant from the US National Science Foundation.

REFERENCES

- 08 1.
Bertin, E. 2010. Astrophysics Source Code Library.
- ¹⁷ The volumetric rate of Giant Flares (as opposed to Hyper-Giant Flares (Equation 20) is off by a factor of 67 relative to the standard FRB volumetric rate (Equation 18).
- ¹⁸ Such optical depths cannot be ruled out for the observed sample of FRBs, given the SNR.
- Bhat, N. D. R., Cordes, J. M., Camilo, F., Nice, D. J., and Lorimer, D. R. 2004, ApJ, 605, 759.
Champion, D. J. *et al.* 2015, ArXiv e-prints.
Condon, J. J., Cotton, W. D., Greisen, E. W., Yin, Q. F., Perley, R. A., Taylor, G. B., and Broderick, J. J. 1998, AJ, 115, 1693.
Connor, L., Sievers, J., and Pen, U.-L. 2015, ArXiv e-prints.
Cordes, J. M. *et al.* 2006, ApJ, 637, 446.
Drew, J. E. *et al.* 2005, MNRAS, 362, 753.
Falcke, H. and Rezzolla, L. 2014, A&A, 562, A137.
Felli, M., Churchwell, E., Wilson, T. L., and Taylor, G. B. 1993, A&AS, 98, 137.

- Ferland, G. J. 2001, *PASP*, 113, 41.
 Gao, H., Li, Z., and Zhang, B. 2014, *ApJ*, 788, 189.
 Gehrels, N., Cannizzo, J. K., Kanner, J., Kasliwal, M. M., Nissanke, S., and Singer, L. P. 2015, *ArXiv e-prints*.
 Hankins, T. H., Kern, J. S., Weatherall, J. C., and Eilek, J. A. 2003, *Nature*, 422, 141.
 Ioka, K. 2003, *ApJ*, 598, L79.
 Karbelkar, S. N. 2014, *ArXiv e-prints*.
 Kasliwal, M. M. 2011. PhD thesis, California Institute of Technology.
 Kasliwal, M. M. and Nissanke, S. 2014, *ApJ*, 789, L5.
 Keane, E. F. and Petroff, E. 2015, *MNRAS*, 447, 2852.
 Keane, E. F., Stappers, B. W., Kramer, M., and Lyne, A. G. 2012, *MNRAS*, 425, L71.
 Klose, S. *et al.* 2004, *ApJ*, 609, L13.
 Kulkarni, S. R., Ofek, E. O., Neill, J. D., Zheng, Z., and Juric, M. 2014, *ArXiv e-prints*.
 Laher, R. R. *et al.* 2014, *PASP*, 126, 674.
 Lang, K. R. 1980, *Astrophysical Formulae. A Compendium for the Physicist and Astrophysicist.*, (Berlin: Springer-Verlag).
 Law, N. M. *et al.* 2009, *PASP*, 121, 1395.
 Loeb, A., Shvartzvald, Y., and Maoz, D. 2014, *MNRAS*, 439, L46.
 Lorimer, D. R., Bailes, M., McLaughlin, M. A., Narkevic, D. J., and Crawford, F. 2007, *Science*, 318, 777.
 Lyubarsky, Y. 2014, *MNRAS*, 442, L9.
 Maoz, D. *et al.* 2015, *MNRAS*, 454, 2183.
 McQuinn, M. 2014, *ApJ*, 780, L33.
 Nissanke, S., Kasliwal, M., and Georgieva, A. 2013, *ApJ*, 767, 124.
 O'dell, C. R. 2001, *ARA&A*, 39, 99.
 Ofek, E. O. 2007, *ApJ*, 659, 339.
 Ofek, E. O. *et al.* 2012, *PASP*, 124, 62.
 Olausen, S. A. and Kaspi, V. M. 2014, *ApJS*, 212, 6.
 Osterbrock, D. E. and Ferland, G. J. 2006, *Astrophysics of gaseous nebulae and active galactic nuclei*, (Sausalito, California: University Science Books).
 Pen, U.-L. and Connor, L. 2015, *ApJ*, 807, 179.
 Petroff, E. *et al.* 2015a, *MNRAS*, 447, 246.
 Petroff, E. *et al.* 2015b, *MNRAS*, 451, 3933.
 Pickles, A. J. 1998, *PASP*, 110, 863.
 Rau, A. *et al.* 2009, *PASP*, 121, 1334.
 Ravi, V., Shannon, R. M., and Jameson, A. 2015, *ApJ*, 799, L5.
 Robitaille, T. P. and Whitney, B. A. 2010, *ApJ*, 710, L11.
 Shannon, R. M. and Johnston, S. 2013, *MNRAS*, 435, L29.
 Spitler, L. G. *et al.* 2014, *ApJ*, 790, 101.
 Tendulkar, S. P., Cameron, P. B., and Kulkarni, S. R. 2013, *ApJ*, 772, 31.
 Thornton, D. *et al.* 2013, *Science*, 341, 53.
 Vachaspati, T. 2008, *Physical Review Letters*, 101(14), 141301.
 Wachter, S., Ramirez-Ruiz, E., Dwarkadas, V. V., Kouveliotou, C., Granot, J., Patel, S. K., and Figer, D. 2008, *Nature*, 453, 626.
 Witham, A. R. *et al.* 2006, *MNRAS*, 369, 581.
 Zheng, Z., Ofek, E. O., Kulkarni, S. R., Neill, J. D., and Juric, M. 2014, *ApJ*, 797, 71.
 Zhou, B., Li, X., Wang, T., Fan, Y.-Z., and Wei, D.-M. 2014, *Phys. Rev. D*, 89(10), 107303.

APPENDIX

A. SIGNAL-TO-NOISE RATIO OF THE BOLOMETRIC FLUENCE

Consider a time series of spectra sampled every δt . Let the frequency range from ν_1 to ν_2 . For instance, for the Arecibo data stream, the frequency range is 1225–1525 MHz (with 960 channels with equal width) and $\delta t = 65.5 \mu\text{s}$ (S14).

Consider the simple case where all the frequency bins are added up with the same weight. For simplicity, assume that the FRB has a width of exactly δt . The bolometric flux is then the sum of the frequency channels. We replace the sum by an integral and find

$$\mathcal{F} = \delta t \int_{\nu_1}^{\nu_2} f(\nu) d\nu \quad (\text{A1})$$

where $f(\nu)$ is the flux density at frequency ν . Assume that $f(\nu)$ is described (in the mean; denoted below by a power law with spectral index α . The mean value (denoted below by $\langle \dots \rangle$) and the variance (denoted by V) of the bolometric fluence is thus

$$\langle \mathcal{F} \rangle = a \delta t \int_{\nu_1}^{\nu_2} (\nu/\nu_2)^\alpha d\nu, \quad (\text{A2})$$

$$V(\mathcal{F}) = \sigma_1^2 (\nu_2 - \nu_1) \delta t^2 \quad (\text{A3})$$

, where a is the flux density at ν_2 and σ_1^2 is the variance per unit frequency (and assumed to be independent of frequency). The basic radiometric equation informs us that $\sigma_1^2 = (T_{\text{sys}}/G)(2\delta t)^{-1}$. Thus, the signal-to-noise ratio (SNR) of the bolometric fluence is

$$\begin{aligned} \mathcal{S} &= \frac{\int_{\nu_1}^{\nu_2} a(\nu/\nu_2)^\alpha d\nu}{\sigma_1 \sqrt{\nu_2 - \nu_1}} \\ &= \frac{a}{\sigma} \frac{\nu_2}{(\alpha + 1)(\nu_2 - \nu_1)} \left[1 - (\nu_1/\nu_2)^{\alpha+1} \right], \end{aligned} \quad (\text{A4})$$

where $\sigma^2 = \sigma_1^2/(\nu_2 - \nu_1)$ is the (traditional) rms for the entire band.

A flat spectrum source has a spectral index of 0 and thus Equation A4 simplifies to a/σ , as expected. A plot of the SNR as a function of α can be found in Figure 9. Notice the loss in SNR with increasing α .

B. OPTIMAL ADDITION OF CHANNELS

We wish to add the detected output from two frequency channels, x_1 and x_2 . Let the statistics of x_k ($k = 1, 2$) be each described by independent Gaussian distribution with means of μ_k and variance, σ_k^2 . Our goal is to find a scheme that maximizes the signal-to-noise ratio (SNR).

Let the optimal statistic be

$$X = \alpha x_1 + (1 - \alpha)x_2. \quad (\text{B1})$$

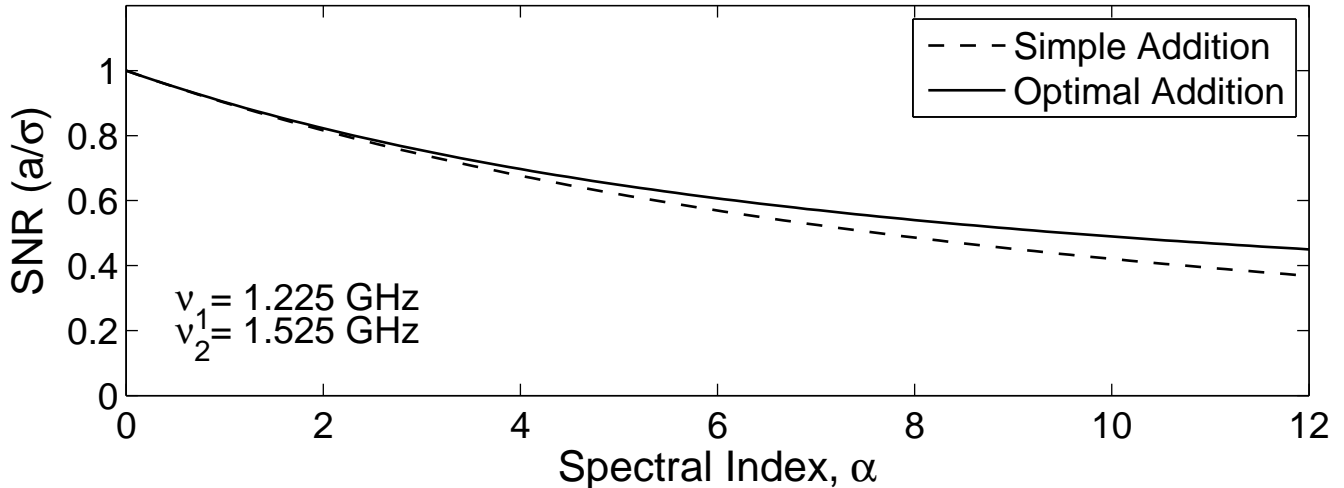


FIG. 9.— Signal-to-noise ratio of the bolometric fluence of a pulse of radiation which has a power law spectrum (power law index, α) over the frequency range $\nu_1 = 1225$ MHz and $\nu_2 = 1525$ MHz. The dashed line is simple addition (Equation A4) and the solid line is the performance of optimal addition (Equation C1).

Note the weights are already normalized, that is the sum of the two weights is unity. The mean value, the variance, and the SNR of X are given by

$$\begin{aligned} \langle X \rangle &= \alpha \mu_1 + (1 - \alpha) \mu_2, \\ V(X) &= \alpha^2 \sigma_1^2 + (1 - \alpha)^2 \sigma_2^2, \\ \text{SNR} &= \frac{\alpha \mu_1 + (1 - \alpha) \mu_2}{\sqrt{\alpha^2 \sigma_1^2 + (1 - \alpha)^2 \sigma_2^2}}. \end{aligned} \quad (\text{B2})$$

SNR is maximized by a judicious choice of α . Differentiating Equation B2 with respect to α yields

$$\alpha = \frac{\mu_1 / \sigma_1^2}{\mu_2 / \sigma_1^2 + \mu_2 / \sigma_2^2}. \quad (\text{B3})$$

The solution to this equation is $\alpha = \mu_1 / (\mu_1 + \mu_2)$. Thus, the weight is proportional to the expected signal strength divided by the variance¹⁹. Substituting this weight into Equation B2 leads to the optimal SNR

$$\text{SNR} = \sqrt{\frac{\mu_1^2}{\sigma_1^2} + \frac{\mu_2^2}{\sigma_2^2}}. \quad (\text{B4})$$

Thus, the optimal SNR is obtained when the SNRs of each measurement is added in quadrature.

C. OPTIMAL EXTRACTION OF THE BOLOMETRIC FLUENCE

We now apply the results of §B to optimally extract the bolometric fluence. The symbols in this section have the same meaning as those in §A.

$$\begin{aligned} \mathcal{S}^2 &= \left(\frac{a}{\sigma_1}\right)^2 \left[\int_{\nu_1}^{\nu_2} (\nu/\nu_2)^{2\alpha} d\nu \right] \\ &= \left(\frac{a}{\sigma_1}\right)^2 \frac{\nu_2}{2\alpha + 1} \left[1 - (\nu_1/\nu_2)^{2\alpha+1} \right] \\ &= \left(\frac{a}{\sigma}\right)^2 \frac{\nu_2}{(2\alpha + 1)(\nu_2 - \nu_1)} \left[1 - (\nu_1/\nu_2)^{2\alpha+1} \right]. \end{aligned} \quad (\text{C1})$$

For the specific case of $\alpha = 0$ we recover the result anticipated on physical grounds, namely $\mathcal{S} = a/\sigma$. The performance of the optimal addition as a function of α is shown in Figure 9. The optimal addition algorithm yields moderately interesting gains only at large values of α .

D. INTEGRATED H α FLUX

The IPHAS photometry, though employing Sloan bands and a custom narrow band H α filter (hereafter, “ ha ”) is tied to Vega magnitude. We will adopt the following zero points: r' (3012 Jy), ha (3012 Jy) and i' (2460 Jy). The

¹⁹ This result is the basis of “matched filter”.

effective bandwidth of the H α filter is 95 Å and thus the flux density integrated over the bandpass of the H α is

$$f(\text{H}\alpha) = 2 \times 10^{-15} 10^{-0.4(ha-20)} \text{ erg cm}^{-2} \text{ s}^{-1}. \quad (\text{D1})$$

Alternatively, we can relate the bandpass integrated flux to the H α magnitude as follows:

$$ha = -2.5 \log \left[\frac{f(\text{H}\alpha)}{2 \times 10^{-7} \text{ erg cm}^{-2} \text{ s}^{-1}} \right]. \quad (\text{D2})$$